Physics of Fluids

The deflection angle between a wind-forced surface current and the overlying wind in an ocean with vertically varying eddy viscosity

Cite as: Phys. Fluids **32**, 116604 (2020); https://doi.org/10.1063/5.0030473
Submitted: 22 September 2020 . Accepted: 02 November 2020 . Published Online: 16 November 2020

Adrian Constantin, David G. Dritschel, and Nathan Paldor

Physics of Fluids ARTICLE scitation.org/journal/phf

The deflection angle between a wind-forced surface current and the overlying wind in an ocean with vertically varying eddy viscosity

Cite as: Phys. Fluids 32, 116604 (2020); doi: 10.1063/5.0030473
Submitted: 22 September 2020 • Accepted: 2 November 2020 •
Published Online: 16 November 2020

Adrian Constantin,[1,a] David G. Dritschel,[2,b] and Nathan Paldor[3,c]

AFFILIATIONS

[1] Faculty of Mathematics, University of Vienna, Vienna 1090, Austria
[2] School of Mathematics and Statistics, University of St Andrews, St Andrews KY16 9SS, United Kingdom
[3] Fredy and Nadine Herrmann Institute of Earth Sciences, The Hebrew University of Jerusalem, Jerusalem 9190401, Israel

[a] adrian.constantin@univie.ac.at
[b] david.dritschel@st-andrews.ac.uk
[c] **Author to whom correspondence should be addressed:** nathan.paldor@mail.huji.ac.il

ABSTRACT

The angle between the wind stress that overlies the ocean and the resulting current at the ocean surface is calculated for a two-layer ocean with uniform eddy viscosity in the lower layer and for several assumed eddy viscosity profiles in the upper layer. The calculation of the deflection angle is greatly simplified by transforming the linear, second-order, vertical structure equation to its associated nonlinear, first-order, Riccati equation. The transformation to a Riccati equation can be used as an alternate numerical scheme, but its main advantage is that it yields analytic expressions for several eddy viscosity profiles.

I. INTRODUCTION

For wind-driven surface ocean currents, various ranges of the deflection angle (i.e., the angle between the current at the ocean surface and the overlying wind that forces it) are recorded.[1] Analytic expressions of the deflection angle are only available for special profiles of vertical eddy viscosities.[2–6] Direct numerical calculations of the transport in the Ekman layer were carried out on a sphere,[7] while the numerical calculations of the deflection angle for depth-dependent eddy viscosity coefficients[8] rely on the WKB approach to find accurate approximations for the solution of the second-order boundary-value problem that governs Ekman flows. The WKB approximation consists of a rapidly oscillating complex exponential multiplied by a slowly varying amplitude and requires that the properties of the medium vary more slowly than the solution.[9] In particular, the eddy viscosity coefficient should vary gradually with depth, an assumption that limits the applicability of the WKB approach.

In this paper, we derive a uniformly valid formula for the deflection angle that, rather than relying on solving a second-order boundary-value problem on an infinite interval, only requires the solution of a first-order initial-value (non-linear) Riccati equation, on a finite interval. The Riccati equation arises in many diverse fields of physics and engineering, e.g., control theory, statistical thermodynamics, quantum mechanics, and cosmology (see the survey in Ref. 10). The transformation of a second-order equation to a Riccati equation has yielded solutions in several recent studies, including Refs. 11 and 12. In light of this, its relevance to the problem of wind-driven ocean currents is, perhaps, not surprising.

II. THE PROPOSED ALGORITHM

The non-dimensional linear governing equations for steady wind-driven ocean currents in mid-latitudes are (see Ref. 6)

$$(K\psi')' - 2\mathrm{i}\psi = 0 \quad \text{for} \quad z < 0, \tag{1}$$

$$\psi'(0) = 1 \quad \text{on} \quad z = 0, \tag{2}$$

$$\psi \to 0 \quad \text{as} \quad z \to -\infty, \tag{3}$$

where the complex vector $\psi = u + iv$ represents the horizontal velocity field, z is the upward pointing vertical variable (with the free surface at $z = 0$) scaled on $\sqrt{(2\tau/\rho)}/f$ (where τ is the applied wind stress at the ocean's surface, ρ is the water density, and f is the constant Coriolis parameter), and $K(z)$ is the vertical depth-dependent, nondimensional, eddy viscosity [which equals the dimensional eddy viscosity scaled on $\tau/(f\rho)$]. Since the turbulence is practically confined to a near-surface ocean layer, it is reasonable to assume that below a certain depth h, the eddy viscosity is equal to the eddy viscosity of sea water, normalized such that

$$K(z) = 1 \quad \text{for} \quad z \le -h, \tag{4}$$

with $K(z) > 0$ for $z \in (-h, 0]$ unconstrained, other than by a continuous dependence on z. The deflection angle from the wind direction at the surface is the argument of the complex vector $\psi(0)$. For $K \equiv 1$, the unique solution to (1)–(3) is

$$\psi(z) = \frac{1}{1+\mathrm{i}}\, \mathrm{e}^{(1+\mathrm{i})z}, \qquad z \le 0,$$

with $\psi(0) = \frac{1}{\sqrt{2}}\, \mathrm{e}^{-\mathrm{i}\frac{\pi}{4}}$ corresponding to a deflection angle of $\frac{\pi}{4}$ (which we will denote below as 45°) to the right of the wind direction; this is the classical result derived by Ekman.[13]

Let us now present the algorithm that we propose for the calculation of the deflection angle for general continuous depth-dependent eddy viscosities; the justification of the procedure is provided in Sec. III.

1. For any given eddy viscosity profile, $K(z)$, solve the Riccati equation

$$q'(z) + \frac{1}{K(z)}\, q^2(z) = 2\mathrm{i} \quad \text{on} \quad (-h, 0), \tag{5}$$

with "initial" data

$$q(-h) = 1 + \mathrm{i}. \tag{6}$$

2. With $q(0)$ computed in step 1, the deflection angle is

$$\arg[\psi(0)] = -\arg[q(0)]. \tag{7}$$

Note that the Riccati equation is essentially the only ordinary differential equation (ODE) admitting a nonlinear superposition principle, a remarkable feature ensuring the existence of a symmetry group and leading to integrability conditions.[14] However, Eq. (5) is not, in general, solvable by quadratures,[15] and in general, one has to rely on numerical methods to obtain accurate approximations of the unique solution to the initial-value problem (5) and (6).

III. METHODS

Let us now justify the algorithm described in Sec. II.

Equation (1) simplifies on $(-\infty, -h)$ to

$$\psi'' = 2\mathrm{i}\psi, \qquad z < -h, \tag{8}$$

for which the general solution is a linear combination of the linearly independent functions $\mathrm{e}^{\pm(1+\mathrm{i})z}$. If we denote by $\psi_\pm$ the solutions of (1) with

$$\psi_\pm(z) = \mathrm{e}^{\pm(1+\mathrm{i})z}, \qquad z < -h, \tag{9}$$

then we have a fundamental system of solutions for (1). The asymptotic behavior (3) thus ensures that the solution ψ to (1) satisfies

$$\psi(z) = C\,\psi_+(z), \qquad z \le 0, \tag{10}$$

for some complex constant C determined by the boundary condition (2). Differentiating (10) and evaluating the outcome and Eq. (10) at $z = 0$, we find

$$\psi(0)\,\psi_+'(0) = \psi_+(0), \tag{11}$$

taking (2) into account. It is known[3] that $\psi(z) \neq 0$ for all $z \le 0$. Consequently, (10) yields $\psi_+(z) \neq 0$ for all $z \le 0$ and $C \neq 0$, while from (10) and (11), we get

$$C = \frac{1}{\psi_+'(0)} = \frac{\psi(0)}{\psi_+(0)}. \tag{12}$$

Now consider the function

$$q(z) = \frac{K(z)\,\psi_+'(z)}{\psi_+(z)}, \qquad z \le 0. \tag{13}$$

From (1), we obtain

$$q'(z) + \frac{q^2(z)}{K(z)} = 2\mathrm{i}, \qquad z < 0,$$

with

$$q(z) = 1 + \mathrm{i}, \qquad z \le -h,$$

due to (9). Consequently, the restriction of the function q to $[-h, 0]$ is the unique solution of the initial-value problem (5) and (6). On the other hand, (11)–(13) yield

$$q(0) = \frac{K(0)}{\psi(0)}. \tag{14}$$

Since $K(0)$ is real, relation (7) emerges. The proposed algorithm is therefore validated.

Remark. The proposed algorithm also yields the horizontal velocity field. Indeed, using (10), integrating (13), and taking (11) and (14) into account, we get

$$\psi(z) = \frac{K(0)}{q(0)}\, \exp\left\{-\int_z^0 \frac{q(s)}{K(s)}\, \mathrm{d}s\right\}, \qquad z \in [-h, 0]. \tag{15}$$

On the other hand, (9), (10), and (12) yield

$$\psi(z) = \frac{\psi(-h)}{\psi_+(-h)}\, \mathrm{e}^{(1+\mathrm{i})z} = \psi(-h)\, \mathrm{e}^{(1+\mathrm{i})(z+h)}, \qquad z < -h,$$

and substituting the expression of $\psi(-h)$ from formula (15) then yields

$$\psi(z) = \frac{K(0)}{q(0)} \exp\left\{(1+\mathrm{i})(z+h) - \int_{-h}^{0} \frac{q(s)}{K(s)}\,\mathrm{d}s\right\}, \quad z < -h. \quad (16)$$

□

IV. EXAMPLES

We now present some examples of solutions to the initial-value problem (5) and (6). Since $K(z) = 1$ for $z \le -h$, it suffices to specify a continuous function K: $[-h, 0] \to (0, \infty)$ with $K(-h) = 1$.

A. The quadratic profile

For the quadratic polynomial

$$K(z) = [a(z+h)+1]^2, \qquad z \in [-h, 0],$$

the substitution $Q(z) = q(z)/(a(z+h)+1)$ transforms (5) and (6) to the equivalent initial-value problem

$$Q'(z) = \frac{2\mathrm{i} - aQ(z) - Q^2(z)}{a(z+h)+1}, \qquad z \in (-h, 0), \quad (17)$$

$$Q(-h) = 1 + \mathrm{i}. \quad (18)$$

To ensure the regularity of $Q(z)$, the values of a and h have to satisfy $ah > -1$. The differential equation (17) is separable and can be straightforwardly integrated, yielding

$$\ln\left(\frac{Q(z) + \frac{a+\zeta}{2}}{Q(z) + \frac{a-\zeta}{2}}\right) = \ln\left(\frac{1+\mathrm{i}+\frac{a+\zeta}{2}}{1+\mathrm{i}+\frac{a-\zeta}{2}}\right) + \frac{1}{a\zeta}\ln[a(z+h)+1], \quad z \in [-h, 0],$$

where

$$\zeta = \sqrt[4]{a^4+64}\,\exp\left[\frac{\mathrm{i}}{2}\arctan\left(\frac{8}{a^2}\right)\right].$$

Since $q(0) = (1-ah)Q(0)$, an explicit formula for the deflection angle (7) emerges, depending on the parameters a and h.

B. The 4/3 power-law profile

For

$$K(z) = [3(z+h)+1]^{\frac{4}{3}}, \qquad z \in [-h, 0],$$

the general solution of (5) is

$$q(z) = -S(z) - (1-\mathrm{i})S^2(z)\tan((1-\mathrm{i})S(z) + C), \qquad z \in [-h, 0],$$

where $S(z) = [3(z+h)+1]^{\frac{1}{3}}$, while C is a complex constant determined by the boundary condition (6). Using the complex identity $\arctan(z) = \frac{1}{2\mathrm{i}}\tan\left(\frac{\mathrm{i}-z}{\mathrm{i}+z}\right)$, we find

$$C = -1 + \mathrm{i} + \frac{\mathrm{i}}{2}\ln\left(\frac{1-\mathrm{i}}{\mathrm{i}-5}\right).$$

C. The linear profile

Previous studies have analyzed the case of an infinitely deep ocean with an eddy viscosity that increases linearly with depth from a value of zero at the free surface.[16] In the present analysis of a surface layer of finite depth (thickness), the linear eddy viscosity profile

$$K(z) = \mu + \frac{\mu - 1}{h}z, \qquad z \in [-h, 0], \qquad \mu > 0,$$

equals μ at the surface and decreases/increases with depth, according to whether $\mu > 1$ or $\mu \in (0, 1)$, respectively. In this case, the general solution of (5) is available in terms of the Bessel functions J_1 and Y_1,[17]

$$q(z) = \frac{2\mathrm{i}h}{\mu - 1}\frac{Q(x)}{Q'(x)}$$

with

$$Q(x) = \sqrt{x}\left[C_1 J_1\left(\zeta\sqrt{x}\right) + C_2 Y_1\left(\zeta\sqrt{x}\right)\right],$$

where C_1 and C_2 are chosen such that their ratio satisfies the boundary condition (6), while $\zeta = 2h(1-\mathrm{i})/(|\mu - 1|)$ and $x = \mu + z(\mu - 1)/h$ ranges between 1 and μ. Note that (6) becomes

$$1 + \zeta\left(\frac{C_1 J_1'(\zeta) + C_2 Y_1'(\zeta)}{C_1 J_1(\zeta) + C_2 Y_1(\zeta)} - 1\right) = 0,$$

which determines the ratio C_1/C_2 purely in terms of ζ; notably, the solution $q(z)$ depends only on this ratio.

V. RESULTS

In this section, we examine how the surface deflection angle θ_0 varies with the value of the surface eddy viscosity $K(0)$ and the depth h of the upper layer of variable eddy viscosity, for the three examples provided in Sec. IV. To gain further insight, we also compare the deflection angle obtained from the associated Riccati equation with the case of constant eddy viscosity in the upper layer that was examined previously in Ref. 6.

The analytical expressions obtained for the three examples above were checked numerically by directly integrating the Riccati equation (5) (a simple `Python` code, entitled "ekman_sipiral.py," which may be adapted for any continuous $K(z)$, is available on zenodo: 10.5281/zenodo.3904295). In most cases, the exact and numerical expressions of $q(z)$ agree within around 10^{-7} (similar to the tolerance of the ODE integrator used). Exceptions occur only when $K(0) \ll 1$, i.e., when (5) is nearly singular at $z = 0$. In the singular case $K(z) \sim -\gamma z$ as $z \to 0$ (here $\gamma > 0$), one can show that to leading order, $q(z) \sim -\gamma/\ln(-z)$ as $z \to 0$, a dependence that is difficult to accurately capture by the ODE integrator without modifying the equation. As this is not an important case, no effort was made to do this.

We start with the 4/3 power law discussed in Sec. IV B since this case depends only on a single parameter, h, and is therefore simplest. The surface deflection angle θ_0 is plotted as a function of h in Fig. 1 (note the log scaling of h). For $h \ll 1$, as expected, $\theta_0 \approx 45°$ since in this case, $K \approx 1$ throughout the shallow upper layer. The largest deflection occurs for $h \approx 2.463$, for which $\theta_0 \approx 62.226\,54°$. At larger depths, the surface deflection angle decreases again, slowly approaching 45° in the limit $h \to \infty$ (which also corresponds to infinite surface eddy viscosity). One can show that $\tan\theta_0 \approx 1 + (3h)^{-1/3}$ for $h \gg 1$.

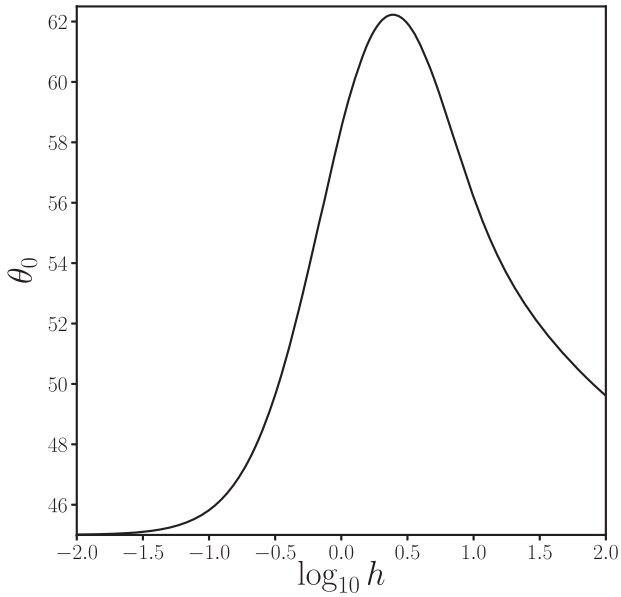

FIG. 1. Surface deflection angle θ_0 (in degrees) as a function of the non-dimensional depth h of the upper layer when $K(z) = [3(z + h) + 1]^{\frac{4}{3}}$ there and $K(z) = 1$ below.

Next, we consider the $K(z) = [a(z + h) + 1]^2$ profile whose analytical solution is provided in Sec. IV A. This now depends on two parameters, a and h. To facilitate comparisons with other profiles of $K(z)$, we use the surface eddy viscosity $K(0) = (ah + 1)^2 \equiv \mu$ as the control parameter instead of a, alongside the upper-layer depth h.

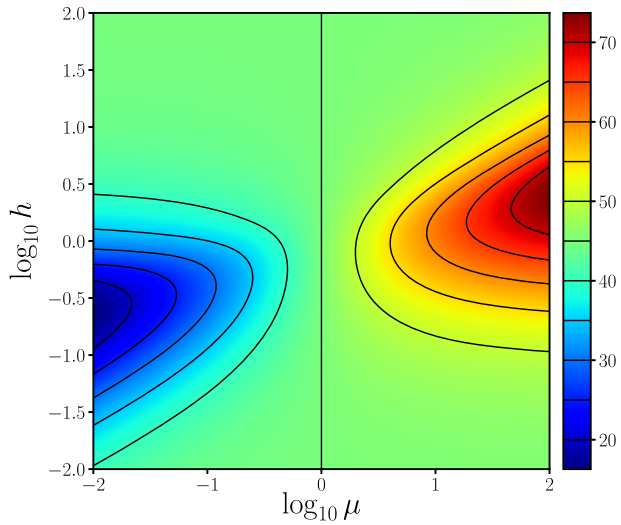

FIG. 2. Contours of the surface deflection angle θ_0 (in degrees) as a function of the surface eddy viscosity μ and non-dimensional depth h of the upper layer when $K(z) = [(\sqrt{\mu} - 1)(z + h)/h + 1]^2$ there.

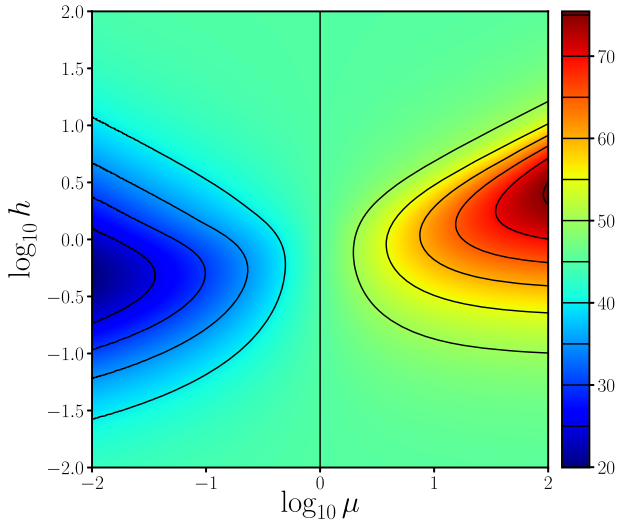

FIG. 3. Contours of the surface deflection angle θ_0 (in degrees) as a function of the surface eddy viscosity μ and non-dimensional depth h of the upper layer when $K(z) = (\mu - 1)(z + h)/h + 1$ there.

The dependence of the surface deflection angle θ_0 on μ and h is shown in Fig. 2 over an extensive range of parameter values. First of all, when $\mu = 1$, $K(z) = 1$ for all z and $\theta_0 = 45°$; this is the constant viscosity case examined originally by Ekman.[13] When $\mu > 1$, the deflection angle is increased, while when $\mu < 1$, it is decreased. The biggest change in θ_0 depends on h, favoring small h when $\mu \ll 1$ and large h when $\mu \gg 1$. In fact, the biggest change occurs roughly on the curve $h = 0.7\mu^{1/4}$, found by a least squares fit to $\log_{10} h = c_0 + c_1 \log_{10} \mu$. While the fit is not perfect, the variance in $\log_{10} h$ is only 0.0175 over the range of $\log_{10} \mu$ considered.

We next examine the linear upper-layer eddy viscosity profile $K(z) = (\mu - 1)(z + h)/h + 1$ introduced in Sec. IV C. The dependence of θ_0 on μ and h is shown in Fig. 3 over the same range of parameter values considered in Fig. 2. The results are broadly similar, with a decrease in θ_0 from 45° for $\mu < 1$ and an increase for $\mu > 1$. For $\mu > 1$, the results compare surprisingly closely, but this is not true for $\mu < 1$, where now the biggest change in θ_0 occurs for larger h, and the same overall change is spread over a larger range of h.

VI. DISCUSSION

The theoretical results derived in this work based on the transformation of the second-order linear differential equation to the associated nonlinear first-order Riccati equation can only be applied to oceanic observation when using a dimensional depth h (or z). As mentioned above, the scale of z equals $\sqrt{(2\tau/\rho)}/f$, so for $\tau = 0.1$ Pa, $\rho = 10^3$ kg/m^3, and $f = 10^{-4}$ s^{-1}, a non-dimensional $h = 1$ corresponds to a dimensional depth of 100 m. Accordingly, the limiting values of $h = 10^{-2}$ and $h = 10^2$ in Figs. 1–3 correspond to dimensional depths of 1 m and 10^4 m, respectively.

In the scaling employed here, the non-dimensional eddy viscosity, $K(z)$, is related to the dimensional viscosity, ν, by $K(z) = \nu\rho f/\tau$. Therefore, the results derived in Subsection IV C for a linear profile

of $K(z)$ with $0 < \mu < 1$ apply equally to a stably stratified mixed layer in the ocean where ν is uniform, but the density, ρ, increases linearly with depth, i.e., when the water temperature decreases linearly with depth. In this commonly observed scenario, the calculations presented in Fig. 3 show that the deflection angle is always smaller than the 45° angle predicted by the classical Ekman solution[13] [which applies when $K(z) = 1$] provided $\mu < 1$. More generally, the variety of stable stratification conditions in the ocean's mixed layer can explain the broad range of deflection angles observed.[1] For uniform density, the results derived in Sec. IV C for $\mu > 1$ yield accurate estimates of the defection angle when ν, the dimensional eddy viscosity, decreases linearly with depth. However, the relevance of these results to the ocean has to be further substantiated since in this case, the mathematical parameter μ has no simple physical counterpart (as is the case for the parameter a in Sec. IV A).

The close relation established by our scaling between the density and the eddy viscosity coefficient of the water further implies that daily and seasonal changes in the temperature of the ocean's mixed layer should alter the deflection angle appreciably. This can explain the poor observational evidence for the 45° value found by Ekman.[13] The deviation of the deflection angle from 45° is encountered even in cases where the observed transport over the entire Ekman layer is consistent with the theoretical estimate.[18] Moreover, since ocean general circulation models include forcing by radiation and other components of the heat budget, our results imply that deviations from the 45° value of the deflection angle should also prevail in numerical simulations. Numerical simulations of the time-dependent wind-forced flow subject to periodic changes in the hydrographic structure of the water column are required to validate this conclusion.

In conclusion, it is instructive to compare the change in the deflection angle that occurs in the piecewise constant case [where $K(z) = \mu$ for $z > -h$ and $K(z) = 1$ for $z \le -h$] when the value of μ varies. The discontinuity of $K(z)$ at $z = -h$ does not permit the use of the proposed Riccati equation algorithm as proposed above. However, a straightforward matching analysis similar to that used in Ref. 6 yields the contour plot of the deflection angle shown in Fig. 4. Notably, a smoothed profile of the eddy viscosity in which $K(z)$ varies continuously near $z = -h$ between the values of μ and 1 [i.e., $K(z)$ varies as $\frac{1}{2}(\mu+1) + \frac{1}{2}(\mu-1)\sin(\pi(z+h)/2\epsilon)$ for $-h - \epsilon \le z \le -h + \epsilon$ with $\epsilon \ll 1$] yields indistinguishable results. These results show that compared to the uniform $K(z)$ associated with $\mu = 1$ in which case $\theta_0 = 45°$, the deflection angle decreases for $\mu \le 1$ provided h is sufficiently small and increases for $\mu \ge 1$ provided h is sufficiently large. Clearly, a simple averaging of the eddy viscosities in the two layers yields an erroneous value of the deflection angle.

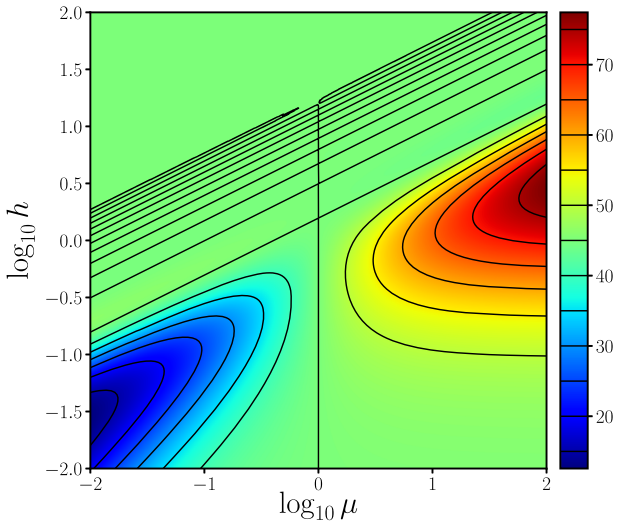

FIG. 4. Surface deflection angle θ_0 (in degrees) as a function of the upper-layer eddy viscosity μ and non-dimensional depth h for a piecewise constant profile of $K(z)$. Here, $K(z) = \mu$ for $z > -h$ and $K(z) = 1$ for $z \le -h$.

DATA AVAILABILITY

Data sharing is not applicable to this article as no new data were created or analyzed in this study.

REFERENCES

[1] J. Röhrs and K. H. Christensen, "Drift in the uppermost part of the ocean," Geophys. Res. Lett. **42**, 10,349–10,356, https://doi.org/10.1002/2015gl066733 (2015).
[2] A. Bressan and A. Constantin, "The deflection angle of surface ocean currents from the wind direction," J. Geophys. Res.: Oceans **124**, 7412–7420, https://doi.org/10.1029/2019jc015454 (2019).
[3] A. Constantin, "Frictional effects in wind-driven ocean currents," Geophys. Astrophys. Fluid Dyn. (published online 2020) .
[4] A. Constantin and R. S. Johnson, "Ekman-type solutions for shallow-water flows on a rotating sphere: A new perspective on a classical problem," Phys. Fluids **31**, 021401 (2019).
[5] A. Constantin and R. S. Johnson, "Large-scale oceanic currents as shallow-water asymptotic solutions of the Navier-Stokes equation in rotating spherical coordinates," Deep Sea Res., Part II **160**, 32–40 (2019).
[6] D. G. Dritschel, N. Paldor, and A. Constantin, "The Ekman spiral for piecewise-uniform viscosity," Ocean Sci. **16**, 1089–1093 (2020).
[7] N. Paldor, "The transport in the Ekman surface layer on the spherical Earth," J. Mar. Res. **60**, 47–72 (2002).
[8] J. O. Wenegrat and M. J. McPhaden, "Wind, waves, and fronts: Frictional effects in a generalized Ekman model," J. Phys. Oceanogr. **46**, 371–394 (2016).
[9] M. H. Holmes, *Introduction to Perturbation Methods* (Springer, New York, 2013).
[10] D. Schuh, "Nonlinear Riccati equations as a unifying link between linear quantum mechanics and other fields of physics," J. Phys. **504**, 012005 (2014).
[11] G. A. Grigorian, "Oscillatory criteria for the second order linear ordinary differential equations," Math. Slovaca **69**(4), 857–870 (2019).
[12] Y. Takey, "Riccati equations revisited: Linearization and analytic interpretation of instanton-type solutions," Complex Anal. Oper. Theory **14**, 78 (2020).
[13] V. W. Ekman, "On the influence of the Earth's rotation on ocean-currents," Ark. Mat. Astron. Fys. **2**, 1–52 (1905).
[14] J. F. Cariñena and A. Ramos, "Integrability of the Riccati equation from a group theoretical viewpoint," Int. J. Mod. Phys. A **14**, 1935–1951 (1999).
[15] E. Hille, *Ordinary Differential Equations in the Complex Domain* (Dover Publication, New York, 1997).
[16] O. S. Madsen, "A realistic model of the wind-induced Ekman boundary layer," J. Phys. Oceanogr. **7**, 248–255 (1977).
[17] A. D. Polyanin and V. F. Zaitsev, *Handbook of Exact Solutions for Ordinary Differential Equations* (CRC Press, Boca Raton, FL, 2000).
[18] T. K. Chereskin, "Direct evidence for an Ekman balance in the California current," J. Geophys. Res.: Oceans **100**, 18261–18269, https://doi.org/10.1029/95jc02182 (1995).